

Polymer Electrolyte Gate Dielectric Reveals Finite Windows of High Conductivity in Organic Thin Film Transistors at High Charge Carrier Densities

Matthew J. Panzer and C. Daniel Frisbie*

Department of Chemical Engineering and Materials Science, University of Minnesota, 421 Washington Avenue SE, Minneapolis, Minnesota 55455

Received March 11, 2005; E-mail: frisbie@cems.umn.edu

Low-voltage operation of organic thin film transistors (OTFTs) is of considerable interest for a variety of inexpensive electronic applications.¹ Because improvements in charge carrier mobility in polymeric and polycrystalline organic semiconductor thin films have begun to plateau around the mobility of amorphous hydrogenated silicon ($1 \text{ cm}^2/\text{V}\cdot\text{s}$),² recent efforts have turned to the development of high capacitance gate dielectric materials to boost OTFT currents and enable lower operating voltages. Materials for increasing the capacitance of OTFT dielectric layers have included high dielectric constant ceramics,^{1a} thin oxides formed by anodization,^{1b} self-assembled monolayer dielectrics,^{1c} and both solid and solution-based electrolytes.³

Attaining very high ($>10^{14}$ charges/ cm^2) carrier densities in OTFTs has not been possible with most dielectric materials due to their relatively low specific capacitance values ($<1 \mu\text{F}/\text{cm}^2$) or the use of narrow voltage ranges to avoid dielectric breakdown. In fact, recent reports of high charge carrier densities achieved in OTFTs typically correspond to only $\sim 2 \times 10^{13}$ charges/ cm^2 .^{1a,c,4} Extremely high charge densities (up to 4.2×10^{17} charges/ cm^2), however, have been obtained in polythiophene electrochemical transistors by the Wrighton group using a liquid SO_2 electrolyte medium as the gate dielectric.^{3g} Interestingly, this group observed finite regions of high hole conductivity (increasing, then decreasing source-drain current with continuously increasing gate voltage) for several polymeric semiconductors when both solution-based and solid polymer electrolyte dielectrics were used.^{3c,g,h}

Here, we report the observation of finite regions of high conductivity in both n- and p-channel OTFTs based on vapor-deposited, polycrystalline organic semiconductor films using a solution-processed, solid polymer electrolyte gate dielectric. OTFTs were prepared by thermal evaporation of either *N,N'*-dioctyl-3,4,9,10-perylene tetracarboxylic diimide (PTCDI-C₈) or pentacene as the organic semiconductor with a spin-coated poly(ethylene oxide) (PEO)/lithium perchlorate polymer electrolyte dielectric as described previously.^{3f} Figure 1 shows a schematic of the device in cross section. The key improvement made to the OTFT architecture since our previous report was the careful alignment of a $200 \mu\text{m}$ wide gold gate (G) electrode to the $200 \mu\text{m}$ channel length (defined by $2000 \mu\text{m}$ wide gold source (S) and drain (D) electrodes), which dramatically lowered leak currents to the gate and allowed us to operate at larger gate voltages.

Figure 2 shows the source-drain current (I_D) and the source-gate current (I_G) versus gate voltage (V_G) measured simultaneously at 295 K for an n-channel PTCDI-C₈ OTFT while sweeping V_G from -0.5 to $+2$ V (forward) and back at a rate of approximately 40 mV/s. All electrical measurements were performed in a temperature-controlled probe station under a $\sim 10^{-6}$ Torr vacuum. The top panel of Figure 2 shows strong device turn-on (large increase in I_D) around $V_G = +0.5$ V, indicating n-channel (electron)

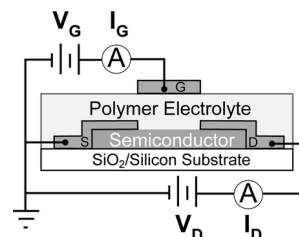


Figure 1. Schematic of a polymer electrolyte-gated OTFT.

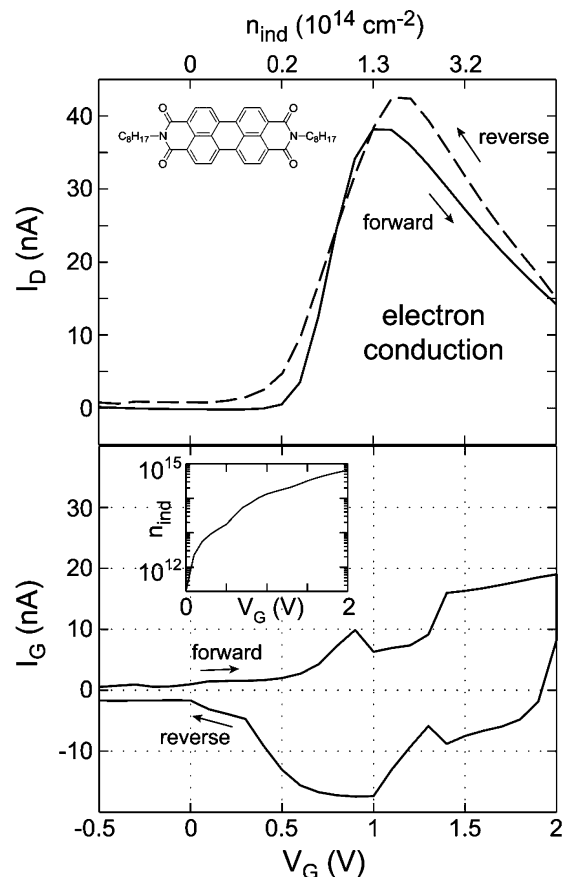


Figure 2. Source-drain current (I_D , top panel) and source-gate current (I_G , bottom panel) versus gate voltage (V_G) measured simultaneously for a PTCDI-C₈ OTFT gated by a polymer electrolyte at 295 K. The source-drain voltage was $+0.5$ V, and the V_G sweep rate was ~ 40 mV/s. Estimated induced electron densities (n_{ind}) were obtained by integrating I_G versus time for the forward sweep. Inset to the lower panel shows the evolution of n_{ind} (charges/ cm^2) with V_G for the forward sweep.

conduction, followed by a clear maximum in conductivity near $V_G = +1$ V and a gradual decrease in I_D as V_G increased from $+1$ to

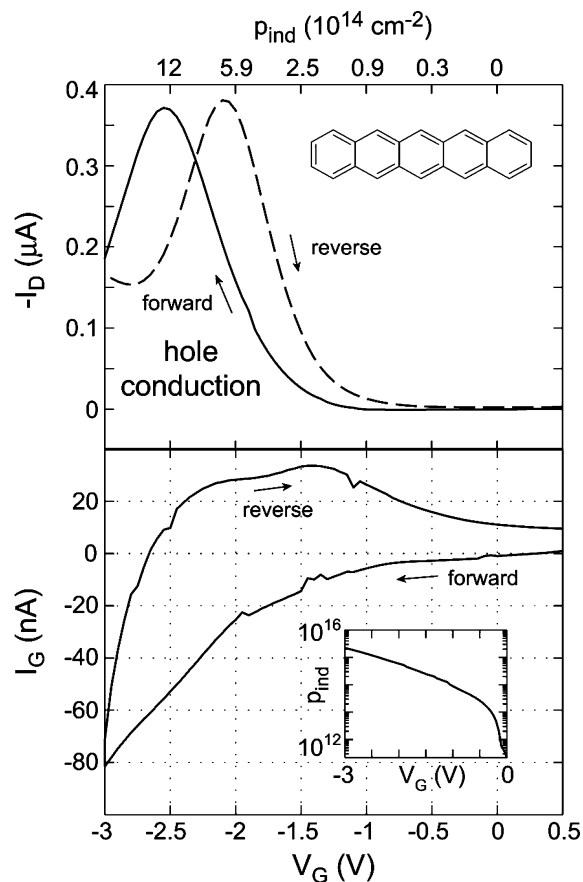


Figure 3. Source-drain current (I_D , top panel) and source-gate current (I_G , bottom panel) measured simultaneously for a pentacene OTFT gated by a polymer electrolyte at 310 K; $V_D = -0.5$ V. V_G was swept at ~ 50 mV/s. Estimated induced hole densities (p_{ind}) were obtained by integrating I_G versus time for the forward sweep. Inset to the lower panel shows the evolution of p_{ind} (charges/cm²) with V_G for the forward sweep.

+2 V. The process that yielded a maximum in I_D appeared to be reversible, as seen in the similar shape of the reverse sweep trace. Additionally, an alternative electrical characterization setup in which both the source and drain currents were monitored individually while sweeping V_G revealed close agreement between the two, indicating that leak to the gate was not responsible for the observed drop in conductivity. Rather, we postulate that the very high degree of reduction (~ 1 e⁻/molecule) achieved with a polymer electrolyte dielectric revealed a reversible transition in the PTCDI-C₈ film from a highly conductive state to a more insulating one.^{3g}

By measuring I_G simultaneously with I_D , we were able to determine the amount of charge induced by the polymer electrolyte dielectric in the semiconductor film directly via integration of I_G versus time, much like cyclic voltammetry. Note that the I_G - V_G characteristic depends on the gate voltage sweep rate; in the limit of sweeping V_G very slow, the transient displacement current (I_G) would decay essentially to zero for a dielectric that did not leak. While it is difficult to make any interpretations at this point of the structure seen in the I_G - V_G characteristic, it is worth pointing out that integration of the forward and reverse I_G sweeps yields approximately the same magnitude of induced charge ($\sim 4.2 \times 10^{-7}$ C), which corresponds to a maximum charge density of $\sim 6.5 \times 10^{14}$ charges/cm² in the OTFT channel at $V_G = +2$ V.

Figure 3 shows the I_D - V_G and I_G - V_G characteristics of a polymer electrolyte-gated pentacene (p-channel) OTFT at a sweep rate of

~ 50 mV/s. An estimated induced hole density of $\sim 2.2 \times 10^{15}$ charges/cm² was reached at $V_G = -3$ V. Again, at approximately $V_G = -2.5$ V on the forward sweep, a maximum in I_D was observed. While increasing the temperature of the system to 310 K for the pentacene OTFT characterization eliminated some of the I_D hysteresis, a delay in the appearance of the maximum in I_D on the reverse sweep indicates that causes of hysteresis remained. This observation, coupled with the relatively slow polarity switch of the pentacene I_G - V_G curve on the reverse sweep in comparison to that of the PTCDI-C₈ OTFT, leads us to propose that some of the hysteresis observed in the case of pentacene could be due to differences in the Li⁺ and ClO₄⁻ transport in the PEO under negative and positive gate bias polarities.

Linear regime mobility values calculated from Figures 2 and 3 are approximately 4×10^{-4} and 3×10^{-4} cm²/V·s for pentacene and PTCDI-C₈, respectively; both higher and lower values than these were observed upon testing of several devices. Since the relatively rough top surfaces of the polycrystalline semiconductor films were gated here, these low mobility values are not surprising. Note that despite the low mobility values, relatively large I_D levels are obtained in the pentacene device because of the very large induced hole concentration. The specific capacitance of the PEO/LiClO₄ polymer electrolyte was found to be an increasing function of the gate voltage, with typical values between 60 and 110 μF/cm² near the maximum in I_D . We anticipate that polymer electrolyte-gated OTFTs can achieve switching speeds of ~ 1 kHz or higher; experiments are underway to test this.

In summary, we have achieved induced charge carrier densities well above 10¹⁴ charges/cm² in polycrystalline n- and p-channel OTFTs gated using a polymer electrolyte dielectric. At very large charge densities, finite regions of high conductivity were observed. A transition in the semiconductor film from a highly conductive state to a more insulating state may be ascribed to the high degree of reduction/oxidation achieved at large charge carrier concentrations; work is ongoing to better understand this phenomenon.

Acknowledgment. M.J.P. thanks the NSF for support provided through a Graduate Research Fellowship. This work was supported primarily by the MRSEC Program of the National Science Foundation under Award Number DMR-0212302.

References

- (a) Dimitrakopoulos, C. D.; Purushothaman, S.; Kymissis, J.; Callegari, A.; Shaw, J. M. *Science* **1999**, *283*, 822–824. (b) Majewski, L. A.; Schroeder, R.; Grell, M. *Adv. Mater.* **2005**, *17*, 192–196. (c) Halik, M.; Klauk, H.; Zschieschang, U.; Schmid, G.; Dehm, C.; Schütz, M.; Maisch, S.; Effenberger, F.; Brunnbauer, M.; Stellacci, F. *Nature (London)* **2004**, *431*, 963–966.
- Dimitrakopoulos, C. D.; Malenfant, P. R. L. *Adv. Mater.* **2002**, *14*, 99–117.
- (a) Lu, C.; Fu, Q.; Huang, S.; Liu, J. *Nano Lett.* **2004**, *4*, 623–627. (b) Siddons, G. P.; Merchin, D.; Back, J. H.; Jeong, J. K.; Shim, M. *Nano Lett.* **2004**, *4*, 927–931. (c) Chao, S.; Wrighton, M. S. *J. Am. Chem. Soc.* **1987**, *109*, 6627–6631. (d) Chao, S.; Wrighton, M. S. *J. Am. Chem. Soc.* **1987**, *109*, 2197–2199. (e) Talham, D. R.; Crooks, R. M.; Cammarata, V.; Leventis, N.; Schloh, M. O.; Wrighton, M. S. *NATO ASI, Ser. B* **1989**, *248*, 627–634. (f) Panzer, M. J.; Newman, C. R.; Frisbie, C. D. *Appl. Phys. Lett.* **2005**, *86*, 103503. (g) Ofer, D.; Crooks, R. M.; Wrighton, M. S. *J. Am. Chem. Soc.* **1990**, *112*, 7869–7879. (h) Ofer, D.; Wrighton, M. S. *J. Am. Chem. Soc.* **1988**, *110*, 4467–4468. (i) Kawarada, H.; Araki, Y.; Sakai, T.; Ogawa, T.; Umezawa, H. *Phys. Status Solidi A* **2001**, *185*, 79–83. (j) Taniguchi, M.; Kawai, T. *Appl. Phys. Lett.* **2004**, *85*, 3298–3300. (k) Hulea, I. N.; Brom, H. B.; Houtepen, A. J.; Vanmaekelbergh, D.; Kelly, J. J.; Meulenkaamp, E. A. *Phys. Rev. Lett.* **2004**, *93*, 166601.
- Naber, R. C. G.; Tanase, C.; Blom, P. W.; Gelinck, G. H.; Marsman, A. W.; Touwslager, F. J.; Setayesh, S.; De Leeuw, D. M. *Nat. Mater.* **2005**, *4*, 243–248.

JA051579+